

# Numerical modelling of internal blast loading on a rock tunnel

Mohammad Zaid<sup>a</sup> and Md. Rehan Sadique<sup>\*b</sup>

*Department of Civil Engineering, ZHCET, Aligarh Muslim University, Aligarh, U.P., India*

*(Received January 8, 2020, Revised April 17, 2020, Accepted May 6, 2020)*

**Abstract.** Tunnels have been an integral part of human civilization. Due to complexity in its design and structure, the stability of underground structures under extreme loading conditions has utmost importance. Increased terrorism and geo-political conflicts have forced the engineers and researchers to study the response of underground structures, especially tunnels under blast loading. The present study has been carried out to seek the response of tunnel structures under blast load using the finite element technique. The tunnel has been considered in quartzite rock of northern India. The Mohr-Coulomb constitutive model has been adopted for the elastoplastic behaviour of rock. The rock model surrounding the tunnel has dimensions of 30 m x 30 m x 35 m. Both unlined and lined (concrete) tunnel has been studied. Concrete Damage Plasticity model has been considered for the concrete lining. Four different parameters (i.e., tunnel diameter, liners thickness, overburden depth and mass of explosive) have been varied to observe the behaviour under different condition. To carry out blast analysis, Coupled-Eulerian-Lagrangian (CEL) modelling has been adopted for modelling of TNT (Trinitrotoluene) and enclosed air. JWL (Jones-Wilkins-Lee) model has been considered for TNT explosive modelling. The paper concludes that deformations in lined tunnels follow a logarithmic pattern while in unlined tunnels an exponential pattern has been observed. The stability of the tunnel has increased with an increase in overburden depth in both lined and unlined tunnels. Furthermore, the tunnel lining thickness also has a significant effect on the stability of the tunnel, but in smaller diameter tunnel, the increase in tunnel lining thickness has not much significance. The deformations in the rock tunnel have been decreased with an increase in the diameter of the tunnel.

**Keywords:** blast load; Coupled-Eulerian-Lagrangian; rock tunnel; concrete liners; Jones-Wilkins-Lee

## 1. Introduction

The scarcity of land area has resulted in the development, construction and utilization of underground spaces in term of tunnels, caverns, storage etc. These underground structures have become an integral part of the modern world. These underground structures play an important role in the transportation of goods and people and are also important for the country's defense program. Underground structures especially, tunnels are vulnerable to blast load in terror attacks such as the Moscow metro tunnel attack in 2010, Saint Petersburg metro tunnel attack in 2017 (Chaudhary *et al.* 2018). During the blast event, tunnel experiences extreme unforeseen load. As these loads are rarely considered in the design, their effects may reduce the serviceability and causing damage to the tunnel and its associated structures. Which develops a major concern to the human life and development authorities. Hence, several researchers had carried out the studies related to blast

---

\*Corresponding author, Professor, E-mail: [rehan.sadique@gmail.com](mailto:rehan.sadique@gmail.com)

effects on different structural components (Kim *et al.* 2018, Kim *et al.* 2018, Vehbi Ozacar, 2018, Jain and Chakraborty 2018, Gang and Kwak 2017, Han and Liu 2016, Wahab and Mazak 2016, Nam *et al.* 2016, Hadianfard *et al.* 2012, Pandey 2010, Ma *et al.* 2009, Nam *et al.* 2009).

A.K. Pandey (2010) carried out a study for the comparison of impact and blast loading on the reinforced concrete (RC) containment shell of a nuclear power plant. The nonlinear response has been studied by using finite element code by validating the study from past literature. Moreover, the dissimilarity between the response of RC due to impact and blast has been studied by incorporating the strain-rate sensitivity analysis. Further, Gang and Kwak (2017) studied the response of concrete beams under blast loading. They have proposed a tension criterion in order to minimize the dependency of results on the finite element meshing. Moreover, the effect of the cross-section of the column on its response during blast loading has been studied by Hadianfard *et al.* (2012) using Ansys software. Moreover, LS-DYNA of Ansys software has also been used for the study of a circular cross-sectional tunnel in saturated soil (Han and Liu 2016). Furthermore, Jain and Chakraborty (2018) utilized finite element software Abaqus for the study of tunnels in the rock. They have studied the performance of basalt fibre reinforced concrete lining in the sandstone rock. Kim *et al.* (2018) carried out the blast study for increasing the serviceability of the warships and, the hardened bulkheads with attached aluminium foam technique has been proposed. Based on 1620 cases of blast study using LS-DYNA software, empirical formulae have been proposed by Kim *et al.* (2018) for masonry brick wall. Further, Ma *et al.* (2009) carried out the study on buried structures under blast loading and focused on the velocity during the event. Nam *et al.* (2009) using LS-DYNA, studied the concrete arch structures for fibre-reinforced polymer retrofitting design. Later, the study was extended to Carbon Fiber Reinforced Plastic (CFRP), and Kevlar/Glass hybrid fabric (K/G) retrofitted reinforced concrete (RC) wall for blast study by Nam *et al.* (2016).

The response of the tunnel under blast loading in rocks is a complex phenomenon due to the presence of structural discontinuities. Due to social, economic and political reasons and the difficulties involving in carrying out the experiment, the experimental study of the tunnel under blast loading is challenging to carry out (Chaudhary *et al.* 2018). Therefore, for the study of the tunnel under blast loading, the numerical methods have to be taken into account to study the tunnel behaviour under blast loading in-depth.

Several researchers using different numerical techniques have studied the behaviour of tunnel under blast load. Yang *et al.* (2010) used the finite element procedure to study the response of the metro tunnel subjected to the above-ground explosion. The response of rock, when subjected to blast load, is governed by its material properties and can be evaluated by the overpressure induced by the blast and particle velocity, as reported by Dowing (1996). Ma *et al.* (1998) has analyzed the damage zone, ground motion and plastic zone due to underground explosion by validating the experimental and numerical results with the assumption of an isotropic, homogeneous, and continuous medium for the study. A continuous damage model for the failure of rock mass was used in the study. Chakraborty *et al.* (2014) investigated the response of different tunnel lining materials using finite element software Abaqus and EOS-JWL model for explosive. Out of single-layered steel plate, plain concrete slab, steel fibre reinforced concrete slab, sandwich steel-dytherm foam-steel panel and steel polyurethane foam-steel panel of lining materials considered, sandwich steel-dytherm foam-steel panel and steel-polyurethane foam-steel panel are found to be the safer as compared to other lining materials. Tiwari *et al.* (2016b) studied the tunnel under blast load in different weathering stages of quartzite rock, using finite element method and CEL approach to model the explosive. It had been found that the fresh Quartzite rock is almost 50 percent safer than

other weathered Quartzite rocks. Further, in fresh rocks, the velocity of blast-induced shock waves was more near-surface in comparison of weathered rocks. Eitzenberger (2012) carried out an experimental and numerical study and concluded that the attenuation of a shock wave is controlled by the texture of rock mass.

Chille *et al.* (1998) used 3D numerical approach to investigate the response of underground electric power plant subjected to blast loading through coupled fluid-solid interaction. However, they had not considered proper interaction between different solid, material nonlinearity and failure criterion. Choi *et al.* (2006) investigated the response of traffic tunnels in rock subjected to blast using 3-D finite element method and coupled fluid-solid interaction. It had been concluded that the blast pressure on the tunnel lining is not the same as the normally reflected pressure obtained using CONWEP (Conventional Weapon) (TM5-1300 1990). Liu (2011) analyzed the tunnel having cast-iron lining using a finite element method for blast loading using CONWEP. Tunnel and cavities subjected to blast load using were investigated through variational difference method by (Feldgun *et al.* 2008a, 2008b).

Liang *et al.* (2013) studied the response of an existing tunnel due to the blast-induced vibrations from an adjacent newly constructed tunnel. Kumar *et al.* (2015) investigated the response of the semi-buried structure under blast loading. The blast loading was applied in the form of the pressure pulse, and the stress-strain response has been simulated by using springs. Nateghi (2012) investigated ground vibration for minimizing negative effects on the surrounding structure due to blast loading. Higgins *et al.* analyzed the plain strain response of tunnel in the sand when subjected to blast loading considering the stress-strain response of soil at high strain rate (Higgins *et al.* 2012).

In brief, the study of rock tunnel under blast load using Coupled-Eulerian-Lagrangian approach (CEL) and Equation of State-Jones Wilkins Lee (EOS-JWL) material model has been rarely studied in the open literature. The present paper considered the Delhi rock tunnel, subjected to blast loading using finite element package Abaqus. The Mohr-Coulomb constitutive model has been adopted for the elastoplastic response of rock. For concrete lining, the concrete damage plasticity (CDP) model has been considered. Trinitrotoluene (TNT) explosive has been used for blast loading. Equation of State method using JWL model has been adopted for TNT. Coupled-Eulerian-Lagrangian modelling has been used to simulate the response of TNT blast loading in the rock tunnel. CEL method is also used for the modelling of air in the tunnel.

Furthermore, the present investigation elaborates the response of rock tunnel when subjected to blast loading under various possible conditions. A combined effect of variation in the following important parameters has been explored.

- (a) depth of overburden
- (b) diameter of tunnel
- (c) amount of TNT and
- (d) thickness of tunnel lining.

## 2. Finite element modeling

A 3D finite element model of rock tunnel and the concrete lining has been developed using lagrangian elements in Abaqus/CAE (Systemes, 2014). Interaction and boundary conditions have been provided using interaction and load modules of the program.

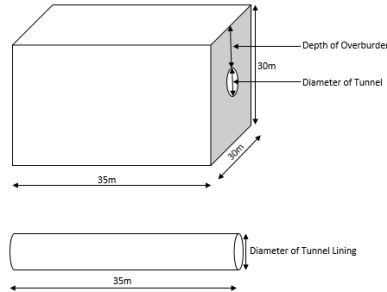


Fig. 1 Geometry of the finite element model

### 2.1 Geometry of the numerical model

The tunnel model has dimensions of 30 m x 30 m and extruded length of 35 m, shown in Fig. 1. The tunnel of different diameter, i.e., 5 m, 6 m, 7 m and 8 m, has been considered in the study. Moreover, the overburden depth on the tunnel has also been varied as 5 m, 7.5 m, 10 m, and 12.5 m. The thickness of tunnel lining has been taken as 0.22 m, 0.35 m, 0.45 m, and 0.55 m in different case studies. However, both lined and unlined tunnels are considered in the present paper.

### 2.2 Constitutive model of rock and lining

The Mohr-Coulomb elastoplastic constitutive model has been considered for the rock. The yield criterion of Mohr-Coulomb plasticity model is given by

$$\tau = c + \sigma \tan \phi \quad (1)$$

where  $\tau$  is shear stress of the rock,  $c$  is the cohesion of the rock,  $\sigma$  is the normal stress, and  $\phi$  is internal friction angle of the rock. For the general state of stress, the model is represented in terms of three stress invariants as

$$F = R_{mc}q - p \tan \phi - c = 0 \quad (2)$$

Where

$$R(\theta, \phi) = \frac{1}{\sqrt{3} \cos \phi} \sin\left(\theta + \frac{\pi}{3}\right) + \cos\left(\theta + \frac{\pi}{3}\right) \tan \phi$$

$$\cos(3\theta) = \left(\frac{r}{q}\right)^3$$

$$p = -\frac{1}{3} \text{trace}(\sigma)$$

$$q = \sqrt{\frac{3}{2} (S:S)}$$

$$r = (9(S * S:S))^{\frac{1}{3}}$$

$$S = \sigma + pI$$

$$G = \sqrt{(\varepsilon c|_0 \tan \psi)^2 + (R_{mw}q)^2} - p \tan \psi \tag{3}$$

Where-

$$R_{mw}(\Theta, e) = \frac{4(1 - e^2) \cos^2 \Theta + (2e - 1)^2}{2(1 - e^2) \cos \Theta + (2e - 1)\sqrt{4(1 - e^2) \cos^2 \Theta + 5e^2 - 4e}} R_{mc} \left( \frac{\pi}{3}, \phi \right)$$

And

$$R_{mc} \left( \frac{\pi}{3}, \phi \right) = \frac{3 - \sin \phi}{6 \cos \phi}$$

Where  $\psi$  is the dilation angle measured in the  $p - R_{mc}q$  plane at high confining pressure,  $c|_0$  is the initial cohesion yield stress,  $c|_0 = c|_{\varepsilon p l} = 0$ ,  $\varepsilon$  is a parameter, referred to as the meridional eccentricity, that defines the rate at which the hyperbolic function approaches the asymptote (this is taken as 0.1 in the present analysis),  $e$  is a parameter, referred to as the deviatoric eccentricity. The deviatoric eccentricity,  $e$ , is calculated as

$$e = \frac{3 - \sin \phi}{3 + \sin \phi} \tag{4}$$

The material properties for the present study are shown in Table 1.

The tunnel lining has been modelled using the concrete damaged plasticity model in Abaqus/CAE (Hibbitt *et al.* 2014). The stress-strain relation of concrete damaged plasticity model is given by

$$\sigma_t = (1 - d_t)D_0^{e1}:(\varepsilon - \varepsilon_t^{e1}) \tag{5}$$

$$\sigma_c = (1 - d_c)D_0^{e1}:(\varepsilon - \varepsilon_c^{e1}) \tag{6}$$

Where, t and c represent tension and compression behaviour, respectively. Here,  $\sigma_t$  and  $\sigma_c$  are tensile and compressive stress vectors, respectively;  $\varepsilon_t^{e1}$  and  $\varepsilon_c^{e1}$  are plastic strains;  $d_t$  and  $d_c$  are the damage variables which are considered functions of plastic strain;  $D_0^{e1}$  is the undamaged initial elastic modulus. The yield function in the concrete damaged plasticity model is given by Lubliner (1989) and later modified by Lee and Fenves (1998)

$$F = \left( \sqrt{\frac{3}{2}} \sqrt{\bar{s}} \right) - 3\alpha\bar{p} + \beta\langle \hat{\sigma}_{max} \rangle - \gamma\langle \hat{\sigma}_{max} \rangle - (1 - \alpha)\bar{\sigma}_c = 0 \tag{7}$$

Where

$$\alpha = \frac{\left( \frac{\sigma_{b0}}{\sigma_{c0}} \right) - 1}{2 \left( \frac{\sigma_{b0}}{\sigma_{c0}} \right) - 1}$$

$$\beta = \frac{\bar{\sigma}_c}{\bar{\sigma}_t} (1 - \alpha) - (1 + \alpha)$$

$$\gamma = \frac{3(1 - K_c)}{2K_c - 1}$$

$$\bar{\sigma}_c = \frac{\sigma_c}{(1 - d_t)}$$

$$\bar{\sigma}_t = \frac{\sigma_t}{(1 - d_t)}$$

Table 1 Input properties of rock (Gupta and Rao 1998, Yadav 2005)

Parameter	Quartzite Rock
Specific Gravity (G)	2.65
Density (kg/m <sup>3</sup> )	2550
Elastic Modulus (GPa)	28
Poisson's Ratio	0.25
The angle of Internal Friction	42°
In situ stress ratio	0.5
Dilation Angle	5°
Cohesion (MPa)	2.3
$\sigma_c$ (MPa)	40
RQD range	75-80
RMR	47

Table 2 Input properties of the concrete lining (Sadique *et al.* 2018)

Parameters	Value
Density (kg/m <sup>3</sup> )	2400
Modulus of Elasticity (GPa)	27.386
Poisson's Ratio	0.17
Dilation Angle (degrees)	30
Eccentricity (constant)	1
Initial equi-biaxial compressive yield stress to initial uniaxial compressive yield stress (constant)	1.16
Second stress invariant ratio, K	0.666
Fracture Energy released (N/m)	720
Uniaxial Failure Stress (Tension) (MPa)	10.8
Cracking Displacement (m)	0.0001332
Tensile Strength (MPa)	3.86
Compressive Strength (MPa)	30

Where,  $\hat{\sigma}_{max}$  is the maximum principal effective stress,  $\bar{s}$  is the deviatoric stress tensor,  $\frac{\sigma_{b0}}{\sigma_{c0}}$  is the ratio of initial equibiaxial compressive yield stress to initial uniaxial compressive yield stress,  $d_t$  is the damage variable and  $K_C$  is the ratio of the second deviatoric stress invariant on the tensile meridian to that on the compressive meridian at initial crushing for any given value of effective mean stress,  $p = \frac{\sigma_1 + \sigma_2 + \sigma_3}{3}$ .

The concrete, damaged plasticity model, assumes a non-associated plastic flow rule. The plastic potential function  $G_P$  used for this model is given

$$G_P = \sqrt{(\varepsilon\sigma_{t0} \tan \psi)^2 + \left(\frac{3}{2}s:s\right)} - \bar{p} \tan \psi \quad (8)$$

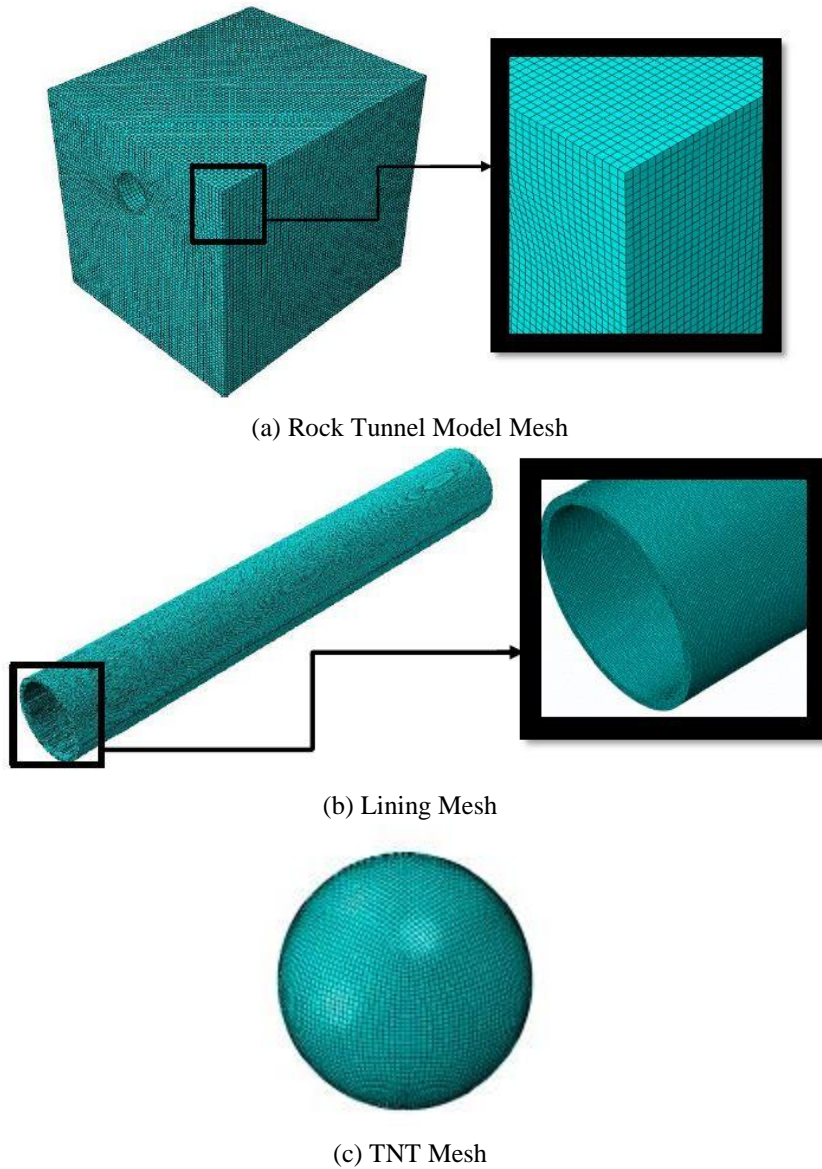
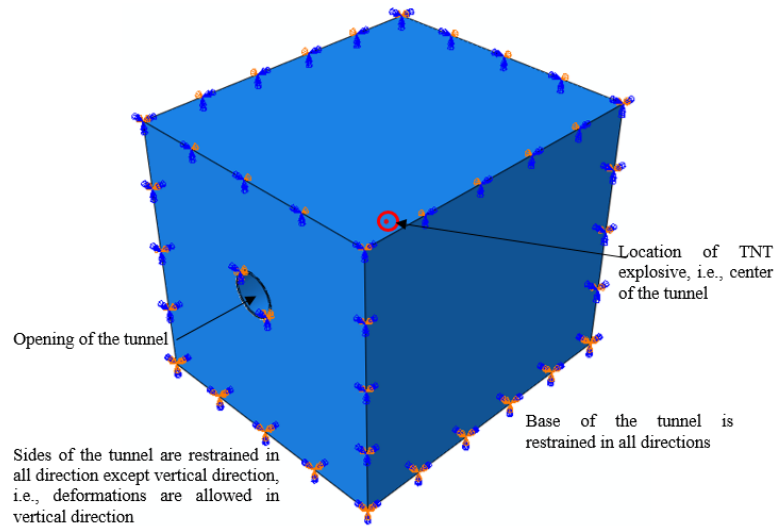


Fig. 2 Meshing of the Model

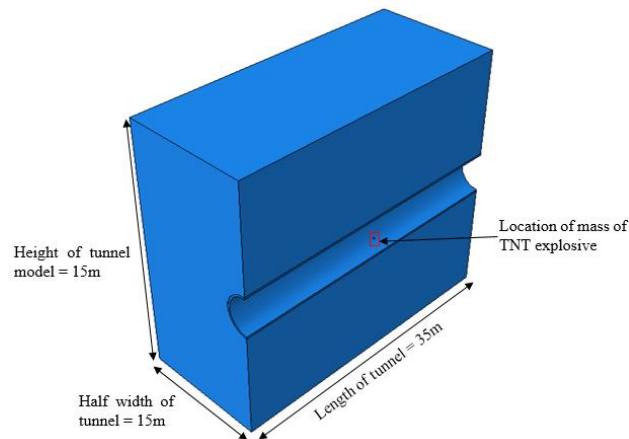
Where  $\psi$  is the dilation angle at mean stress-deviatoric stress plane;  $\sigma_{t0}$  is the uniaxial tensile stress at failure, the value of which is set by the user and  $\varepsilon$  is the eccentricity parameter. If the eccentricity is zero, the potential plastic function becomes a straight line. The concrete damage plasticity parameter values are shown in Table 2.

### 2.3 Meshing and element type

The Lagrangian element mesh has been applied through the 3D part module in Abaqus/CAE to



(a) Full model



(b) Half model

Fig. 3 Boundary Conditions of the Model

develop FE models of rock and concrete lining. An eight-noded brick element (C3D8R) with reduced integration, hourglass control and finite membrane strains has been adopted to obtain the structured mesh of the model. The model has been discretized through the mesh convergence study. 1.25 m, 1.10 m, 1 m, 0.8 m, 0.6 m, 0.4 m, 0.2 m, 0.1 m, 0.08 m, 0.06 m, 0.04 m, 0.02 m, 0.01 m, and 0.005 m were the different mesh sizes adopted in the optimization of element size and number of elements. For these different size elements, the magnitude of deformation increases with decrease in the element size. Therefore, by comparing the magnitude of deformation at the centre of the tunnel length, it has been concluded that 0.02 m size of the element is the most optimized. A typical simulation took about 12 CPU hours on Dell Precision Tower 7810 Workstation with Xeon processor E5-2600v4 and 64GB RAM. Moreover, 5mm element size has been used to mesh the TNT Eulerian sphere. The meshing of different components of the model

Table 3 Input properties for JWL material for TNT explosive (Larcher and Casadei 2010)

Density (kg/m <sup>3</sup> )	Detonation Wave Speed (m/s)	A (MPa)	B (MPa)	$\omega$	R <sub>1</sub>	R <sub>2</sub>	Detonation Energy Density (kJ/kg)
1630	6930	373800	3747	0.35	4.15	0.9	3680

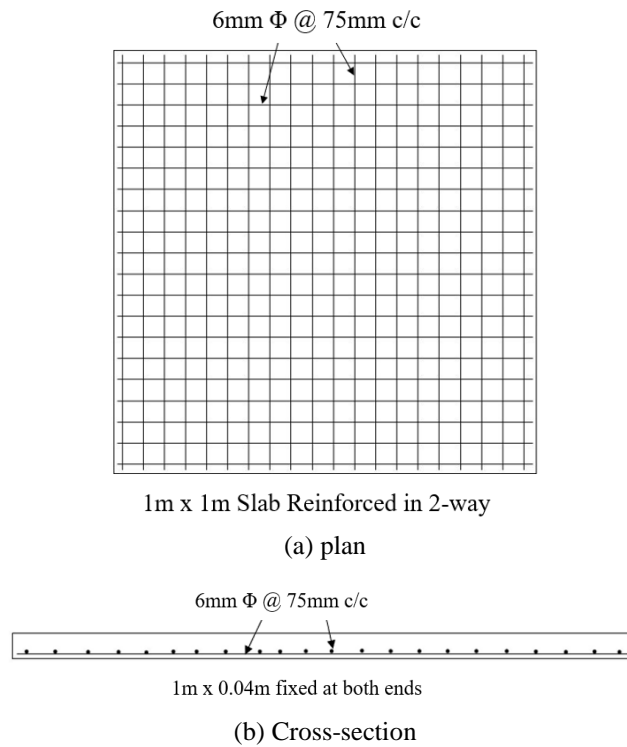


Fig. 4 Concrete Slab

has been shown in Fig. 2. The general contact applied to the model as contact between tunnel lining and rock. It provides hard contact in the normal direction and frictionless contact in the tangential direction.

### 2.5 Coupled-Eulerian-Lagrangian (CEL) Modeling of Air and TNT explosive

The Coupled-Eulerian-Lagrangian modelling technique has been used to model the Air and TNT explosive. As Eulerian material can flow through the lagrangian mesh, this technique has been used for the present study (Tiwari *et al.* 2016a). The CEL modelling provides a powerful platform for the simulations involving the generation of high stresses and strains in the elements. The Eulerian continuum 3D eight noded reduce integration elements EC3D8R has been used for CEL modelling. In CEL modelling, the Eulerian Volume Fraction (EVF) tool is used for filling the Eulerian elements with material either fully or partially. The material fraction can be tracked by EVF tool, wherein, EVF=0, represents an entirely void element and EVF=1 represents elements filled with material. In the present study, EVF =1 has been used for explosive modelling, which is

filled with a Eulerian element having zero voids. However, the air has been modelled by using  $EVF = 0.8$ , having 20% voids. The boundary of Eulerian material may not match with the element geometry as the material flows through the Eulerian mesh and hence, has to compute at each time instant. After the explosion, loss of air from a Eulerian grid may lead to a reduction in accuracy of analysis due to loss of kinetic energy. Hence, the larger size of the grid containing Eulerian elements has been considered in order to prevent the loss of air. For the proper interaction between Eulerian and Lagrangian elements, the general hard contact has been defined between explosive, air, tunnel lining surfaces. The smallest element size of 20 mm has been used for meshing based on mesh convergence study.

Jones-Wilkins-Lee material model has been considered for the modelling of Trinitrotoluene in Abaqus. The pressure ( $p$ ) for the TNT explosive can be calculated using the Jones-Wilkins-Lee (JWL) equation of state (EOS) (Larcher and Casadei 2010) as given

$$p = A \left( 1 - \frac{\omega}{R_1 \bar{\rho}} \right) e^{-R_1 \bar{\rho}} + B \left( 1 - \frac{\omega}{R_2 \bar{\rho}} \right) e^{-R_2 \bar{\rho}} + \omega \rho e_{int}$$

Where,  $A$ ,  $B$ ,  $R_1$ ,  $R_2$  and  $\omega$  are material constants for TNT explosive.

- $A$  and  $B$  =magnitudes of pressure,
- $\bar{\rho}$  = ratio of the density of the explosive in the solid-state ( $\rho_{sol}$ ) to the current density ( $\rho$ )
- $e_{int}$  = specific internal energy at atmospheric pressure.

High pressure generated during an explosion is represented by the first two exponential terms represents, and the last term is a low-pressure term, which deals with high volume due to explosion in the JWL equation of state. The input properties of TNT are shown in Table 3.

### 3. Validation of CEL Finite element model

For validation of the numerical approach used in this research, results have been compared with the experimental studies available in the open literature. Zhao and Chen (2013) had carried out an experimental investigation to demonstrate the mechanism and mode of damage of a square reinforced concrete slab subjected to blast loading. The square reinforced concrete slab having dimensions of 1 m x 1 m x 0.4 m has been cast, as shown in Fig. 4 (Zhao and Chen 2013). The displacement of two sides of the slab has been restrained in all the directions, as espoused in the experimental setup. The reinforcement has 6 mm diameter and was placed at 75 mm centre to centre in both the directions. 20 mm cover has been provided for the reinforced concrete slab. The slab has a cylindrical compressive strength of 39.5 MPa, tensile strength of 4.2 MPa, and Young's modulus of concrete of 28.3 GPa. The reinforcement has Young's modulus of 200GPa and yield strength of 600 MPa. The slab has been subjected to three different blast loads of 0.2 kg, 0.31 kg and 0.46 kg at a scaled distance of  $0.684 \text{ m/kg}^{1/3}$ ,  $0.591 \text{ m/kg}^{1/3}$  and  $0.518 \text{ m/kg}^{1/3}$  respectively. The CEL method of modelling has been used to model TNT blast loading.

The experimental and numerical results of Zhao and Chen (2013) can be found at Fig. 12 of Zhao and Chen (2013) and Fig. 10 and Fig. 11 of Wang *et al.* (2013) and results of present validation has been compared in Table 4. The maximum deformation reported in the present study is in proximity. The deformation contours for the numerical validation of the experimental study of Zhao and Chen (2013) were shown in Fig. 5.

Table 4 Validation of Deformation at the center of the slab

Explosive Charge (kg)	Deformation at the center of the panel (mm)		
	Zhao and Chen (2013)		Present Paper
	Experimental Study	Numerical Study	Numerical Study
0.2	10	8.8	8.15
0.31	15	12.7	12.25
0.46	35	31.1	29.91

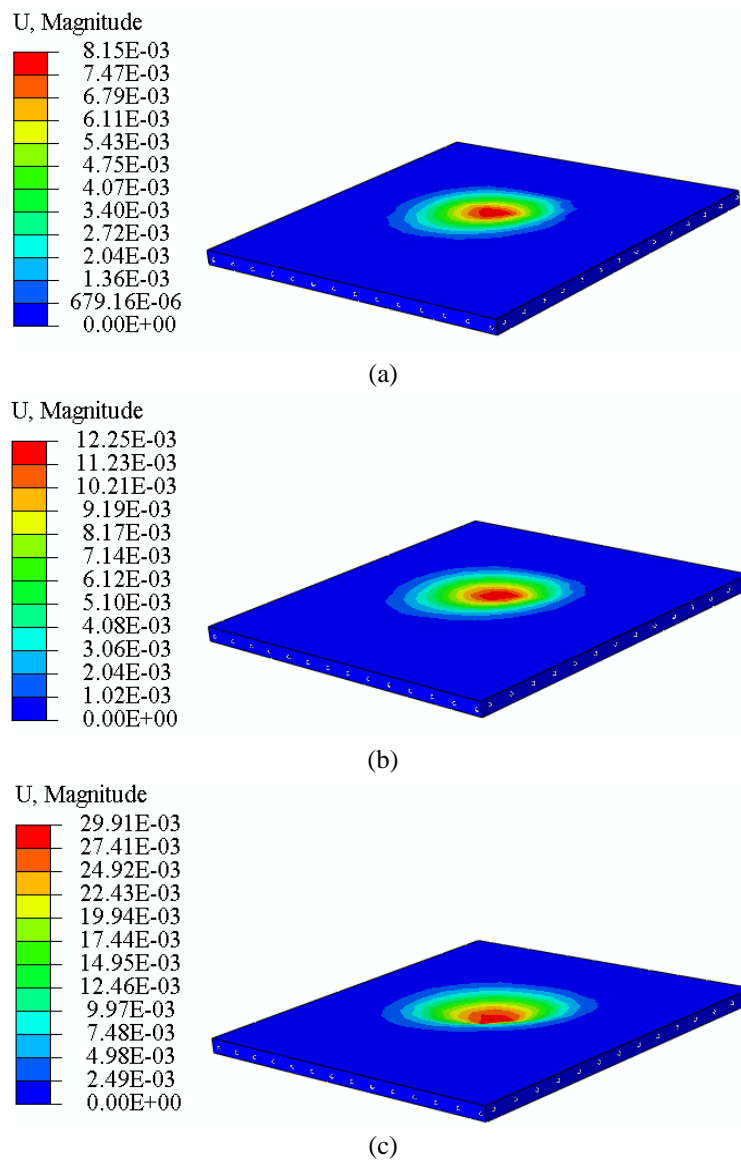


Fig. 5 Deformation Contours for Validation of Reinforced Slab Subjected to Blast Loading, (a) 0.2 kg, (b) 0.31 kg and (c) 0.46 kg TNT mass

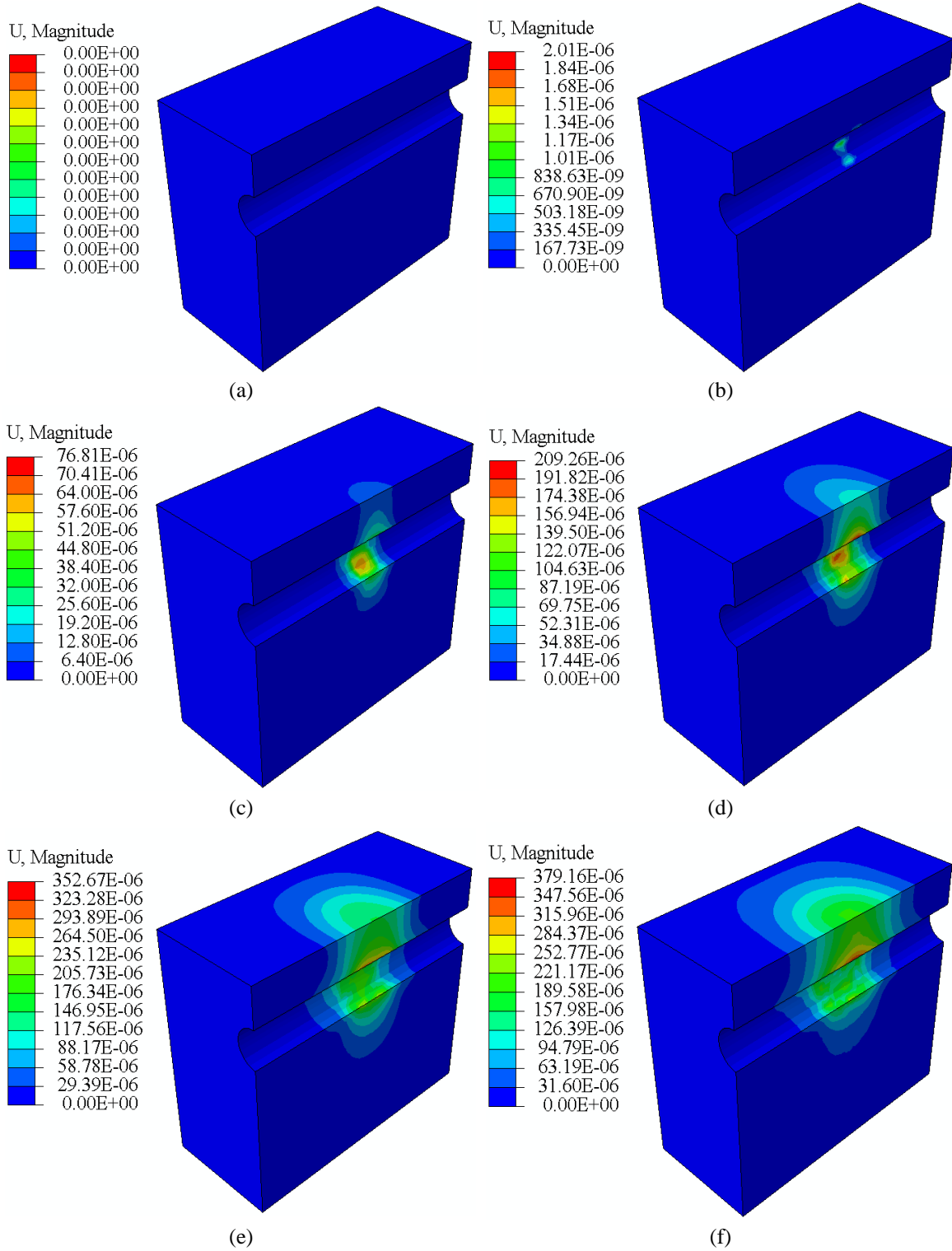


Fig. 6 Continued

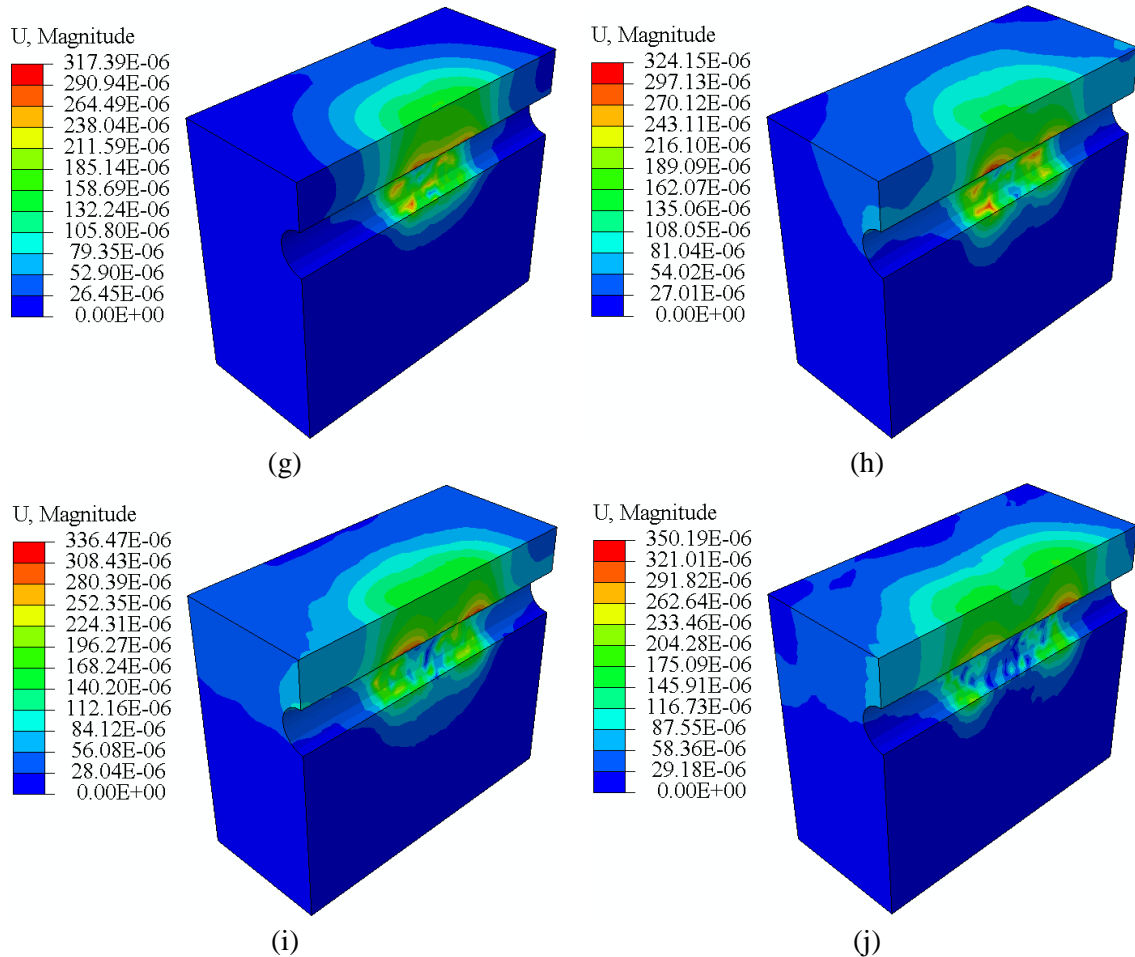


Fig. 6 Deformation contours at different time frames for 5 m diameter tunnel having 5 m overburden depth and 0.22 m liner thickness when subjected to 30 kg TNT explosive (a) 0s, (b) 0.003s, (c) 0.006s, (d) 0.009s, (e) 0.012s, (f) 0.015s, (g) 0.018s, (h) 0.021s, (i) 0.024s and (j) 0.027s

#### 4. Results and Discussions

A three-dimensional finite element analysis has been carried out using finite element software Abaqus/Explicit. A rock tunnel model has been developed and analyzed under the blast loading due to TNT explosive. The blast occurrence time was assumed to be 60 ms (millisecond), as the maximum deformation almost reached within this time. Further, the parametric study has been carried out by varying the depth of overburden, the diameter of the tunnel, for lined and unlined tunnels under the loading of TNT explosive. Moreover, the tunnel lining thickness has also been varied. In brief, the following parameters have been varied in the simulation to observe the behaviour of the tunnel under different circumstances.

- (a) The diameter of the tunnel: 5 m, 6 m, 7 m and 8 m
- (b) Thickness of lining: 0.22 m, 0.35 m, 0.45 m and 0.55 m
- (c) The mass of TNT explosive: 10 kg, 20 kg, 30 kg, 40 kg, 50 kg, and 60 kg

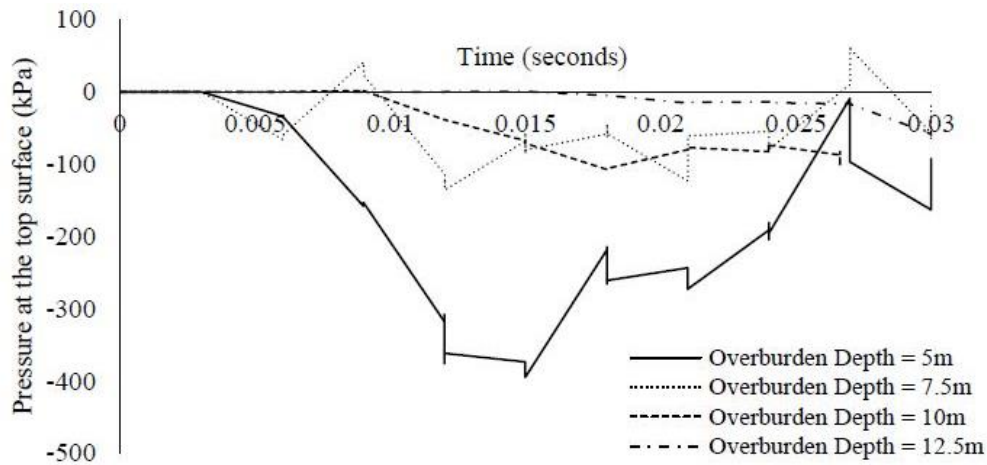


Fig. 7 Variation of pressure due to 30kg TNT explosive for different overburden depths of the tunnel with time for 0.22 m of liner thickness 5m diameter of the tunnel at the ground surface

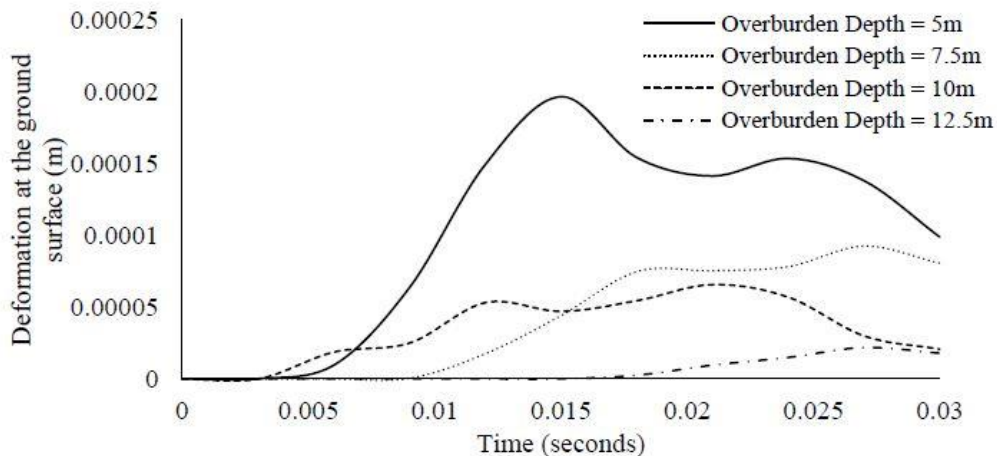


Fig. 8 Variation of deformation due to 30 kg TNT explosive for different overburden depths of the tunnel with time for 0.22 m of liner thickness 5 m diameter of the tunnel at the ground surface

(d) The overburden depth of tunnel: 5 m, 7.5 m, 10 m and 12.5 m

In Fig. 6, deformation contours are presented at different periods to show the response of a tunnel during an event of blast loading. It has been noted that as the blast event initiates, the deformation was transferred from the internal surface of the tunnel to the ground surface. Moreover, the larger length of the tunnel has been damaged with time due to heat and blast waves of the explosive. Further, it has been observed that the higher value of deformation will be noted at structures constructed above the tunnel surface. Underground structures undergo three primary modes of deformation during seismic shaking: compression-extension, longitudinal bending and ovaling/racking. However, in blast loading, the deformation is localized, and expansion of tunnel may occur due to heat generated during the blast event; however, the study of heat generation is not a part of the present study.

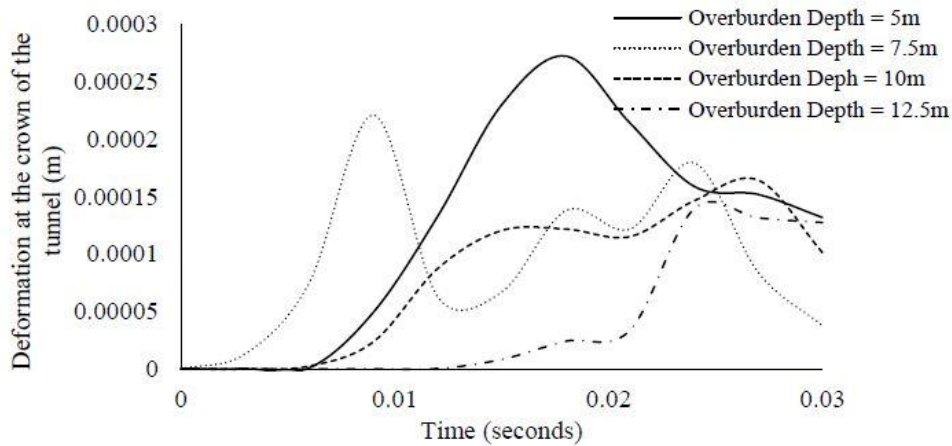


Fig. 9 Variation of deformation due to 30 kg TNT explosive for different overburden depths of the tunnel with time for 0.22 m of liner thickness 5 m diameter of the tunnel at the crown of the tunnel

Fig. 7 has been plotted to understand better the nonlinear response of the rock tunnel during the blast loading in the internal of tunnel lining. From the Fig. 7, it has been noted that higher value of pressure has been observed at a shallow depth of tunnel whereas the value of pressure decreases with increase in overburden depth at the ground surface of the tunnel. Moreover, a rapid decrease in pressure has been observed for change in overburden depth from 5 m to 7.5 m. After which the decreasing value of pressure is noted, but the change in values is not significant.

Additionally, the plots of deformation variation with time are shown in Fig. 8 at the ground surface when the tunnel has been subjected to internal blast loading of 30 kg TNT explosive for different overburden depths. In case of shallow depth of 5 m, significant damage to the tunnel has been observed, while lower deformations are observed at the ground surface, as the overburden depth tends to increase. Therefore, the structures constructed at the shallow depth of the tunnel are more prone to failure due to internal blast loading in the tunnel as compared to the case of deep tunnels.

Fig. 9 has been plotted for the variation of the deformation with the time, which were noted at the crown of the tunnel. The constant blast loading due to 30 kg TNT explosive has been considered in the 5 m diameter tunnel having 0.22 m of liner thickness. By comparing different overburden depth of the rock tunnel, it has been observed that the peak of deformation varies with the overburden depth and value of deformation shows a decline in the value with increasing depth of the tunnel. Moreover, the maximum deformation in the different cases has concluded that deeper tunnels are safer than shallow tunnel in rocks.

Figs. 10 (a) - 10(d) shows the deformation in rock vs weight of TNT explosive for different tunnel lining thickness. Each plot is for different tunnel diameter but under constant overburden depth, i.e., 12.5 m. Fig. 10 (a), 10(b), 10(c) and 10(d) represents the plot for tunnel having a diameter of 5m, 6m, 7m and 8m, respectively. With the increase in weight of TNT, the maximum reported deformation in a rock has been increasing, as expected, in each case. Fig. 10(a) shows the plot of deformation in rock subject to varying explosive load for 5m diameter tunnel. No significant decrease in deformation may be observed through an increase in liner thickness for this diameter

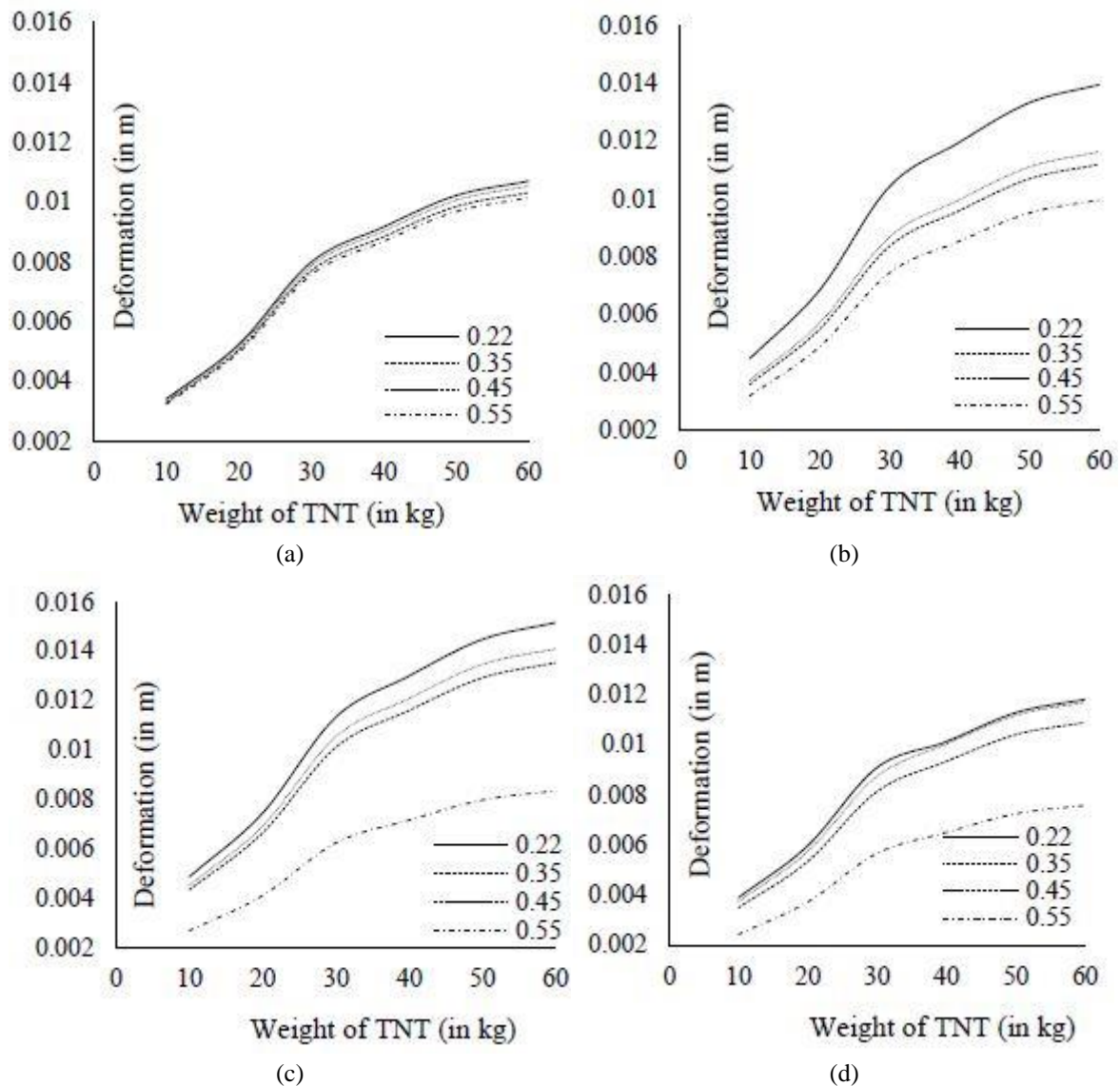


Fig. 10 Effect of tunnel lining thicknesses under a different mass of TNT explosive for a 12.5 m deep tunnel having a diameter of (a) 5 m, (b) 6 m, (c) 7 m and (d) 8 m

of the tunnel. However, for tunnels of bigger diameter, there is a decrement in the deformation in rock as the thickness of tunnel lining increases. As the diameter of the tunnel increases the distance between the TNT charge and the concrete lining increases, which reduces the deformation in the tunnel lining. The profile of deformation vs weight of TNT charge shows non-linear behaviour. It also shows that the deformation vs weight of TNT profile differentiated clearly with an increase in diameter of tunnel lining.

The CDP model in Abaqus is used for incorporating the damage in the concrete lining. It provides general capability in the modelling of concrete. Moreover, the CDP model uses the

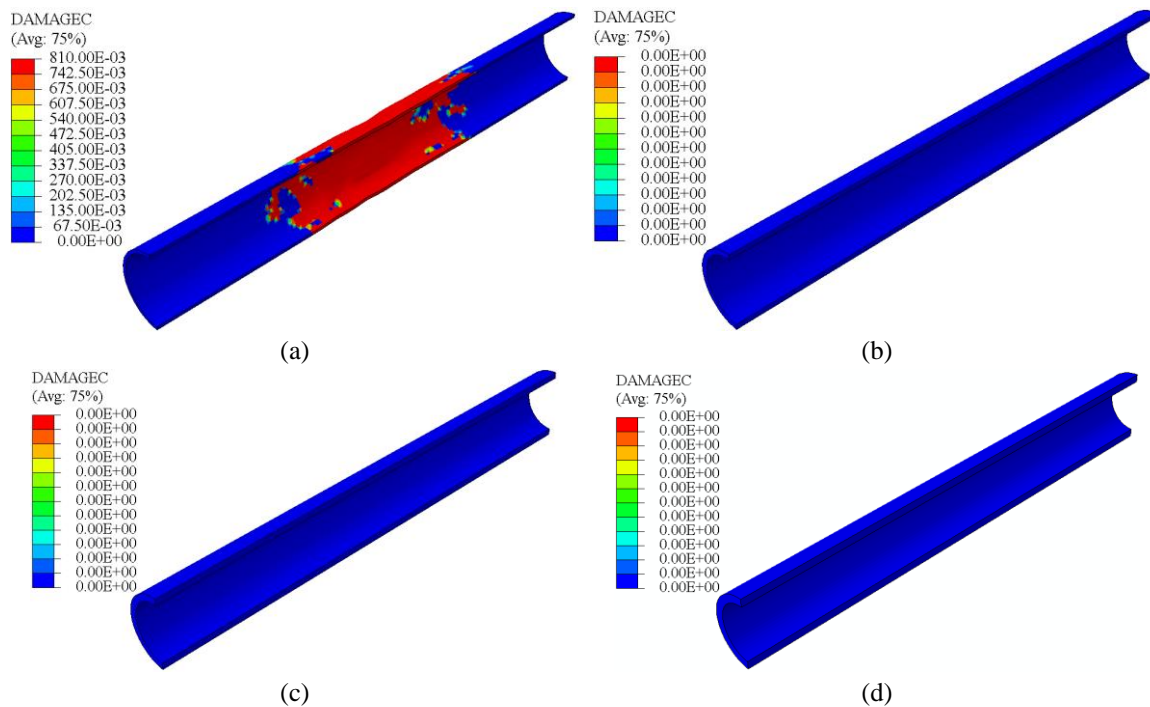


Fig. 11 Compression damage contours of different tunnel lining thickness (a) 0.22 m, (b) 0.35 m, (c) 0.45 m and (d) 0.55 m in case of 5m diameter tunnel having 5 m overburden depth when 30 kg TNT explosive has been assumed as charge at internal of the rock tunnel

isotropic tensile and compressive plasticity behaviour concept of isotropic damaged elasticity to represent the inelastic behaviour of concrete. The CDP model can also be incorporated in the analysis for plain concrete. The damage contours of different concrete liners are presented in Figs. 11 and 12 for the compression and tension damage respectively, when 30 kg TNT blast has been assumed to act of explosive charge. The compression damage in the 0.22 m concrete liner has a maximum failure. Almost, one-third length of the concrete liner has the failure at the middle of tunnel length. Moreover, the concrete liner thickness has been increased and proved advantageous in overcoming the compression damage in the concrete liner. Therefore, in term of compression damage, 0.35 m of liner thickness is the most suitable choice for an underground tunnel as blast-resistant design. Similarly, in case of tension damage also, the 0.22 m of concrete liner thickness is the most unsuitable choice. Besides, 0.35 m of concrete liner prove to be sufficient and an economical choice out of the considered cases. When a blast load from a TNT charge having 30 kg weight acts, 2-3 m of concrete liner gets damage. Therefore, while comparing the tension damage with compression damage, it has been observed that concrete liner is having 0.22 m of thickness damaged 6-times in compression than in tension failure. Further, it has been noted that the damage of the concrete liner is not a matter of concern if the concrete liner has thickness value higher than 0.22 m. Furthermore, the health of the tunnel remains excellent and sound for concrete liner thickness of 0.35 m, 0.45 m and 0.55 m. From this, it is concluded that an economical and serviceable choice of the concrete liner has to be adopted while designing the underground rock tunnels for blast-resistance.

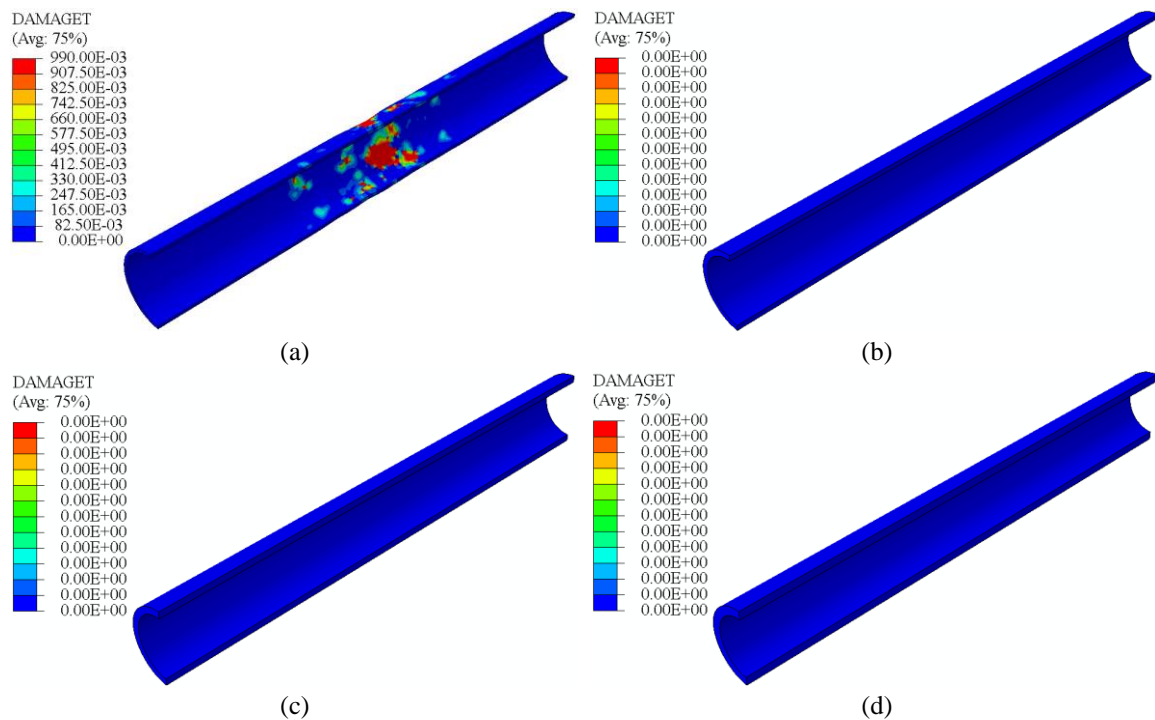


Fig. 12 Tension damage contours of different tunnel lining thickness (a) 0.22 m, (b) 0.35 m, (c) 0.45 m and (d) 0.55 m in case of 5 m diameter tunnel having 5 m overburden depth when 30 kg TNT explosive has been assumed as charge at internal of the rock tunnel

Figs. 13(a) - 13(d), shows the graphs for the comparison of different diameter tunnels under the varying load of TNT explosive for each tunnel lining thicknesses, having constant 5 m depth of overburden. The response of 0.55 m tunnel liner thickness has been being plotted for comparing the effect of tunnel diameter in Fig. 13(a). Similarly, Fig. 13(b), 13(c) and 13(d) were plotted for tunnel liner thickness of 0.45 m, 0.35 m and 0.22 m, respectively. It has been observed that with the increase in TNT loading, the deformation also increases, but in the curvilinear pattern. However, the gradient is falling sharply with the increase in the mass of explosive. When the TNT explosive increases from 10 kg to 20 kg, the deformation increases by 61%, for 20 kg to 30 kg by 66%, for 30 kg to 40 kg by 14%, for 40 kg to 50 kg by 10%, and 50 kg to 60 kg by 5%. This behaviour has a similar pattern for all diameters of tunnels having varying tunnel lining thickness.

When the strain is mentioned in engineering problems, it is the ratio of change in length from the initial to final value to the original length. However, logarithmic strain takes into account the continuous variation of length with time depending upon the material. Moreover, the logarithmic strain is the most suitable parameter for materials having a smaller part of strain in the elastic range. Fig. 14 shows the colour contours of logarithmic strain in different cases of overburden depth. The shallow depth tunnel having 5 m of overburden has a higher value of stains, thus making it the most venerable case of rock tunnel. However, the logarithmic strain value decreases with the increase in the overburden depth of the tunnel. It has been observed that for shallow rock tunnel, the logarithmic strain (for 5 m depth of overburden) is  $102.4 \times 10^{-6}$  and  $63.66 \times 10^{-6}$  is the logarithmic strain for 7.5 m depth of overburden. For an increase in depth of overburden from 5 m

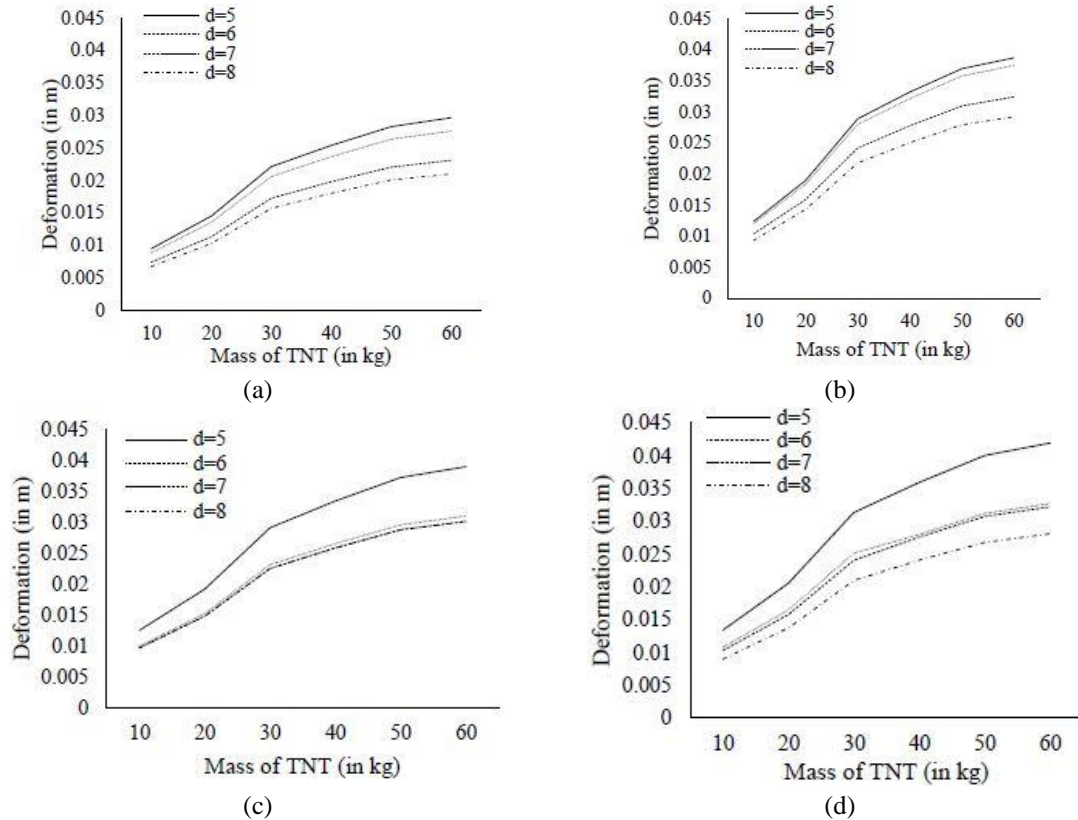


Fig. 13 Comparison of different diameter tunnels under the load of varying mass of TNT explosive for having (a) 0.55 m, (b) 0.45 m, (c) 0.35 m, and (d) 0.22 m thickness of tunnel lining having 5 m depth of overburden

to 7.5, the logarithmic strain value decreases by 62%, leading the tunnel towards safety. Similarly, as the depth of overburden increases from 10 m to 12.5, the logarithmic strain has decreased by 3.8-times. Thus, rock tunnel having higher overburden depth are more resistant to blast loads as compared to shallow overburden depth tunnel.

The response of all liners has been plotted under different overburden depths, with varying the mass of TNT, Figs. 15(a) - 15(d). The comparison of different overburden depth has been plotted for each thickness of tunnel liner. Fig. 15 (a), 15(b), 15(c), and (d) are plotted for 0.55 m, 0.45 m, 0.35 m and 0.22 m respectively. It has been found that with an increase in the depth of overburden, the deformation in the rock decreases, which has a logarithmic relation with TNT mass. A similar trend has been observed for other, tunnel lining thickness and overburden depth combinations.

Analysis has also been performed for the unlined tunnel. The deformation caused in the unlined tunnel by different mass of explosive has been shown in Fig. 16. Fig. 16(a) represents the response for overburden depth of 5m and tunnel diameter has been varied. Similarly, Fig. 16(b), 16(c) and 16(d) were the response curve of the tunnel having 6m, 7m and 8m diameter, respectively. All graphs in Fig. 16 shows a nonlinear increase in deformation when subjected to increasing TNT explosive from 10 kg to 60 kg. For the tunnel having 8 m diameter and 5 m overburden depth,

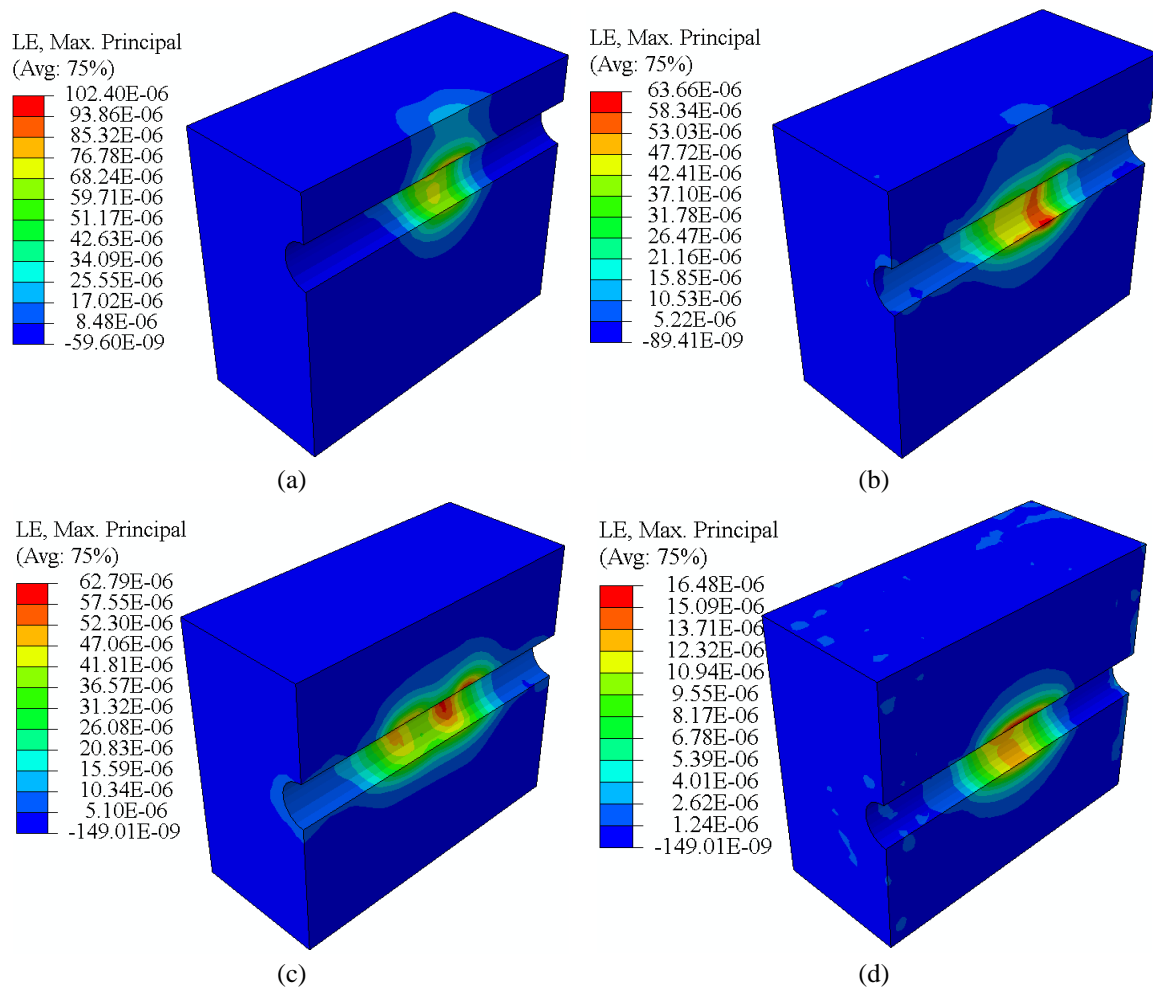


Fig. 14 Logarithmic Strain in different overburden cases (a) 5 m, (b) 7.5 m, (c) 10 m and (d) 12.5 m when subjected to 30 kg TNT explosive

with the increase in loading of TNT explosive from 10 kg to 60 kg at an interval of 10 kg the deformation increases by 65% - 66% for each interval.

The deformation contours for the comparison of different diameter tunnels having 0.22 m thickness of tunnel lining and 5 m depth of overburden when subjected to the load of 60 kg TNT, as shown in Fig. 17. With the increase in the diameter of the tunnel, the deformation in the rock tunnel decreases. However, maximum deformation has been very localized in small diameter and widely extended in case of a bigger tunnel. Nevertheless, quantitatively the maximum deformation has been observed in the 5m diameter tunnel, and the minimum deformation has been observed for 8m diameter tunnel, i.e., 19.48 mm and 9.48 mm, respectively. Further, comparing the effect at the ground surface, the deformation has been decreased by 26% in the case of 5 m diameter tunnel and 4% in rest of the cases.

The deformation profile for the comparison of different depths of overburden has been plotted in Fig. 18. For this plot, 5 m length of the tunnel has been considered along with the crown of the

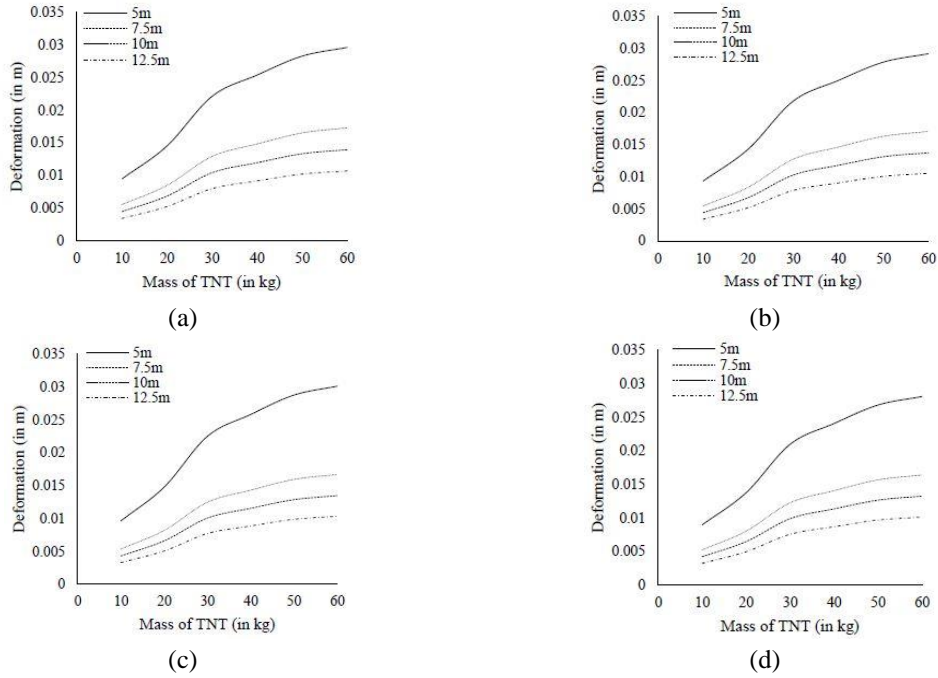


Fig. 15 Comparison of different overburden depth under a load of varying mass of TNT explosive for 5 m diameter tunnel having (a) 0.55 m, (b) 0.45 m, (c) 0.35 m and (d) 0.22 m tunnel lining thickness

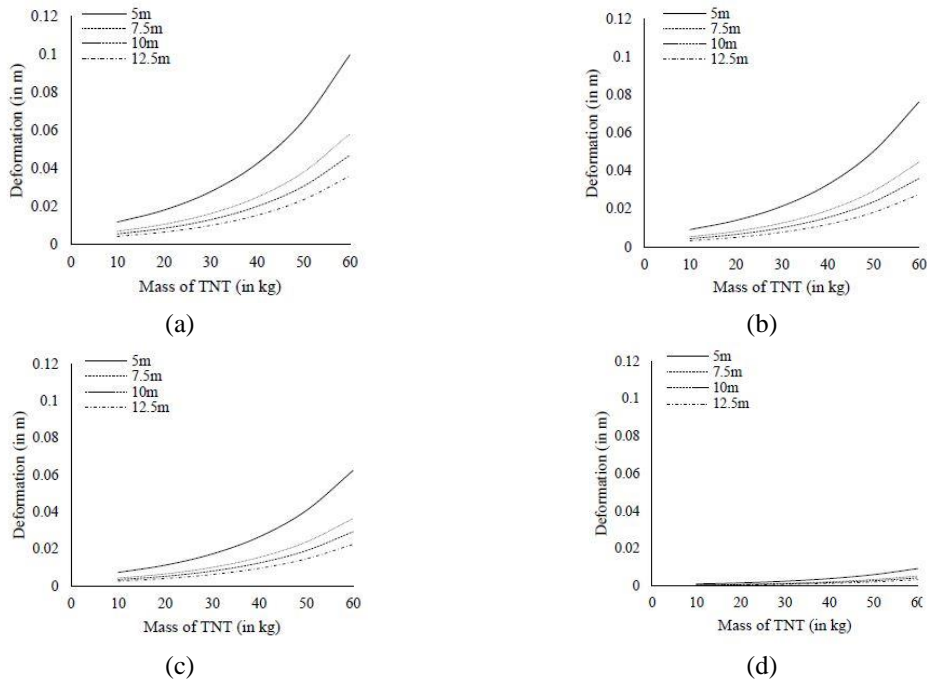


Fig. 16 Comparison of different depth of overburden for varying mass of TNT explosive (a) 5 m, (b) 6 m, (c) 7 m and (d) 8 m diameter unlined tunnel

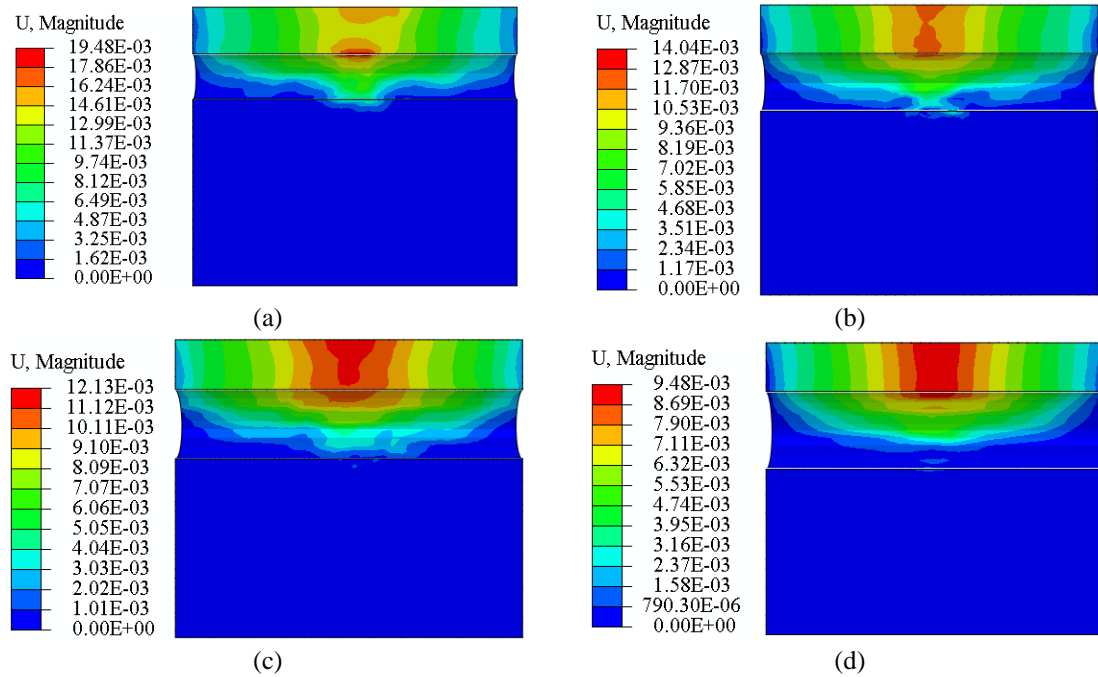


Fig. 17 Deformation contours for (a) 5 m, (b) 6 m, (c) 7 m and (d) 8 m of the diameter of the tunnel for 5 m overburden depth and 0.22 m lining thickness under a load of 60 kg TNT explosive

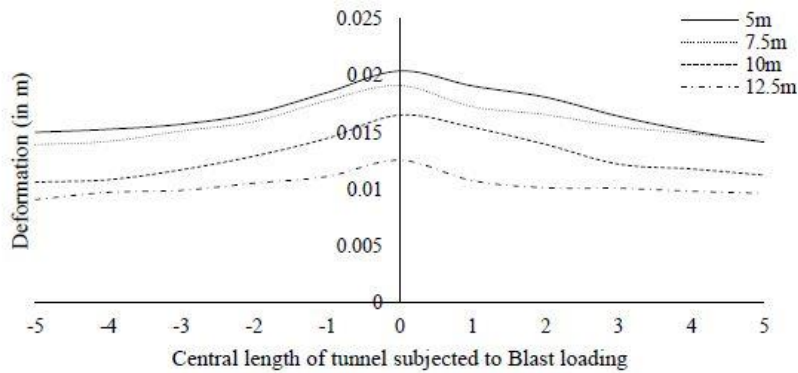


Fig. 18 Deformation profile for different depth of overburden under a load of 60 kg TNT explosive mass for 5 m diameter tunnel and 0.55m tunnel lining thickness (at the time of maximum deformation in the tunnel)

tunnel both front and rear side from the origin. Where origin has been coinciding with the centre of TNT mass. It has been observed that when a tunnel is subjected to TNT explosive loading, the surface just above the TNT experiences heavy loading and the surface bulges upwards. The deformation diminishes as we move away from the blast location along the longitudinal axis of the tunnel. However, this phenomenon was more visible in shallow depth tunnel.

To understand the failure and serviceability of the underground rock tunnel Mises stress (also known as von Mises stress) is an important parameter. The Mises stress gives an idea about the

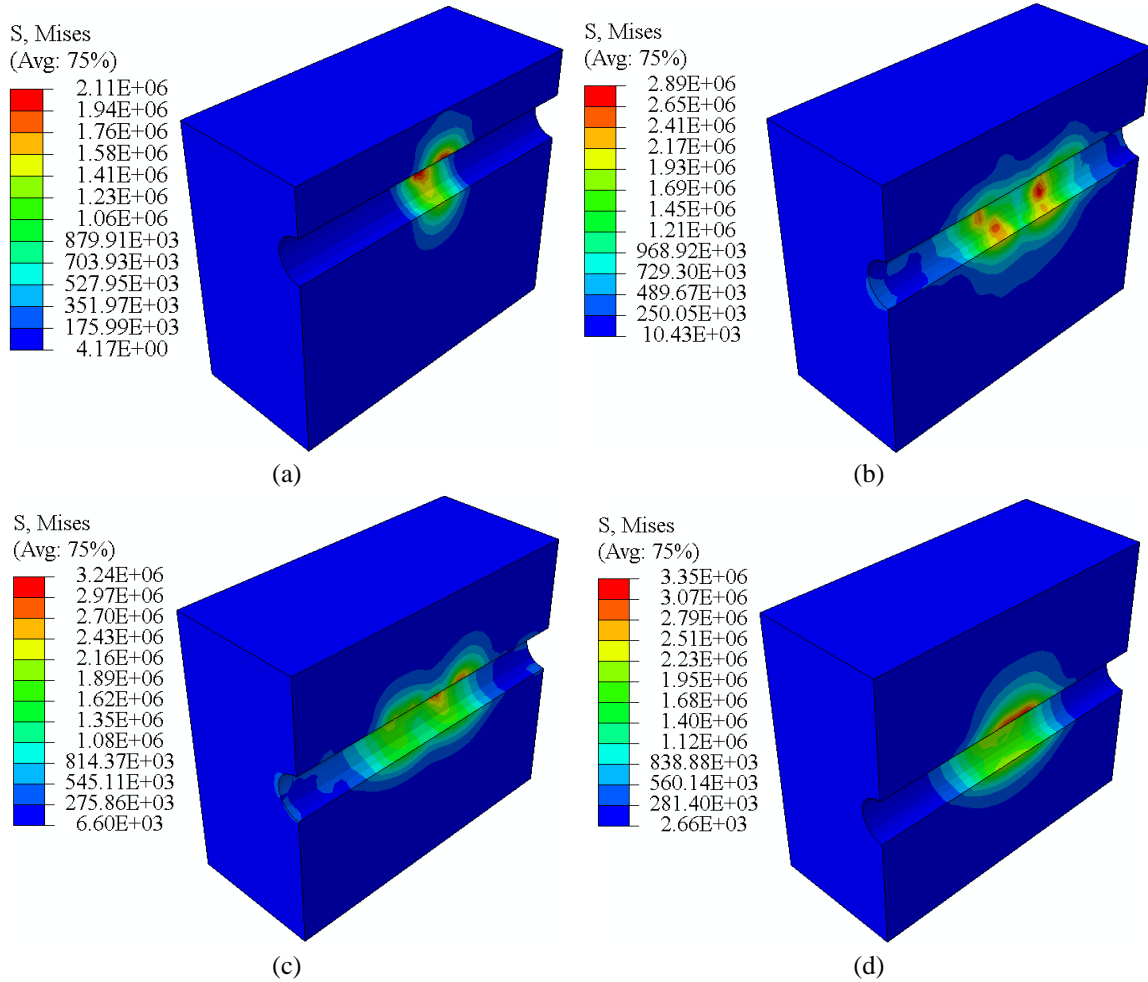


Fig. 19 Mises stress contours for the comparison of overburden depth of tunnel having 5 m diameter and 0.22 m thickness of tunnel liner when subjected to 60 kg TNT explosive

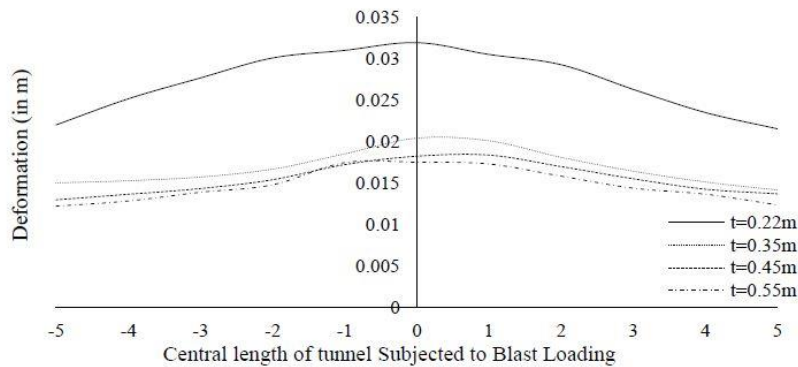


Fig. 20 Deformation profile for different tunnel lining thickness under a load of 60 kg TNT explosive mass for 5 m depth of overburden and 5 m diameter tunnel (at the time of maximum deformation in the tunnel)

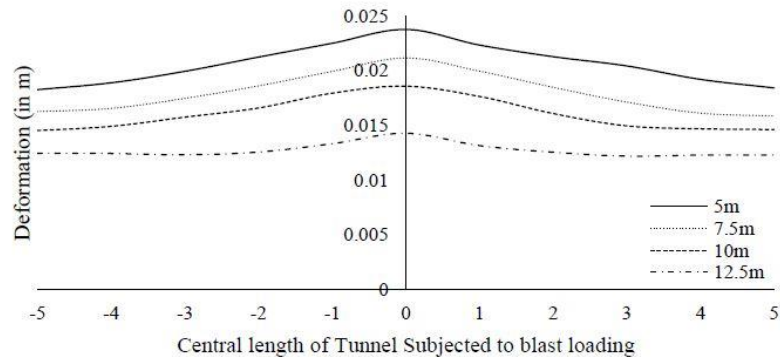


Fig. 21 Deformation profile for different depth of overburden under a load of 60 kg TNT explosive mass for 5 m diameter *unlined* tunnel (at the time of maximum deformation in the tunnel)

fracture of the material. Therefore, a comparison of the Mises stress is an essential component for nonlinear analysis; therefore, Fig. 19 has been plotted for the comparison of stresses in different cases of overburden depth. Minimum Mises stress is observed for shallow tunnel having 5 m of the depth of overburden, i.e., 2.11 MPa. Further, the value of Mises stress has increased with an increase in depth of overburden. Therefore, Lower value of Mises stresses has been observed in shallow overburden depth of 5 m, and the maximum value of Mises stress has been observed for 12.5 m depth of overburden having value as 3.35 MPa.

The deformation profile has been plotted in Fig. 20 for the comparison of different tunnel lining thickness for 5 m diameter tunnel having 5 m depth of overburden when subjected to 60 kg TNT. It may be concluded that with an increase in the thickness of tunnel lining the deformation reduces. However, the reduction in deformation was very less, after a particular increase in the thickness of the tunnel lining. Thus, increasing the thickness of concrete liner became less significant in the blast resistant design of the tunnel.

For the comparison of different depths of overburden for unlined tunnels under the loading of 60 kg TNT for the tunnel having 5 m diameter, the deformation profile has been shown in Fig. 21. For the unlined tunnels, the deformation behaviour is similar to the lined tunnel, but as the depth of overburden increases the deformation profile becomes a straight line. Hence, shows linear behaviour of deformation profile. Thus, a stage will reach when there is the negligible effect of blast loading on the rock tunnel.

## 5. Conclusions

3D finite element analysis has been carried out to study the response of underground rock tunnel constructed in quartzite rock. Both the lined and unlined rock tunnels have been taken into account. The finite element software Abaqus has been adopted for the present paper. Four parametric studies have been carried out in the present paper, for overburden depth, the diameter of the tunnel, the thickness of tunnel lining and amount of explosive (TNT).

The paper concludes that deformations in lined tunnels follow a nonlinear pattern, and in unlined tunnels, a linear pattern has been observed. The stability of the tunnel has increased with an increase in the depth of overburden in lined and unlined tunnels. However, the deformation

profile shows a linear pattern in case of unlined tunnels and nonlinear pattern in case of lined tunnels. The tunnel lining thickness also has a significant effect on the stability of tunnel but in smaller diameter tunnel, the increase in tunnel lining thickness has not much consequence. The deformations in the rock tunnel have been decreased with an increase in the diameter of the tunnel, and maximum deformation has been very localized in small diameter and widely extended in case of a bigger tunnel. With an increase in the amount of TNT explosive, an exponential increase in deformation has been observed in case of unlined tunnels, and a nonlinear pattern has been noted in case of lined tunnels.

In term of net damage and post-blast health of the tunnel, it may be concluded that liner thickness greater than 35 mm is safe for all the amount of TNT charge considered in the present study. Nevertheless, significant deformation and surface settlement may occur, depending upon other size and depth of tunnel.

## Acknowledgements

Authors would like to acknowledge Mr. Manojit Samanta, Senior Scientist (CBRI-CSIR Roorkee, U.K., India) for assisting in computational facility.

## References

- A. Eitzenberger (2012) *Wave propagation in rock and the influence of discontinuities*. Lulea University of Technology, Sweden.
- A.K. Pandey (2010), "Damage prediction of RC containment shell under impact and blast loading", *Struct. Eng. Mech.*, **36**(6), 729-744, <https://doi.org/10.12989/sem.2010.36.6.729>.
- C. H. Dowing (1996), *Construction vibrations*. Trowbridge: Prentice-Hall Englewood Cliffs Comite Euro-International du Beton, Redwood Books.
- Chakraborty, T., Larcher, M. and Gebbeken, N. (2014), "Performance of tunnel lining materials under internal blast loading", *Int. J. Protective Struct.*, **5**(1), 83-96. <https://doi.org/10.1260/2041-4196.5.1.83>.
- Chaudhary, R.K., Mishra, S., Chakraborty, T. and Matsagar, V. (2018), "Vulnerability analysis of tunnel linings under blast loading", *Int. J. Protective Struct.*, **10**(1), 1-22. <https://doi.org/10.1177/2041419618789438>.
- Chille, F., Sala, A. and Casadei, F. (1998), "Containment of blast phenomena in underground electrical power plants", *Advan. Eng. Software*, **29**(1), 7-12. [https://doi.org/10.1016/S0965-9978\(97\)00047-1](https://doi.org/10.1016/S0965-9978(97)00047-1).
- Choi, S., Wang, J., Munfakh, G. and Dwyre, E. (2006), "3D Nonlinear blast model analysis for underground structures", *GeoCongress 2006*. [https://doi.org/10.1061/40803\(187\)206](https://doi.org/10.1061/40803(187)206).
- D. Systemes (2014), *Abaqus 6.14 Documentation*. Providence, RI: Dassault Systèmes.
- Feldgun, V.R., Kochetkov, A.V., Karinski, Y.S. and Yankelevsky, D.Z. (2008a), "Blast response of a lined cavity in a porous saturated soil", *Int. J. Impact Eng.*, **35**(9), 953-966. <https://doi.org/10.1016/j.ijimpeng.2007.06.010>.
- Feldgun, V.R., Kochetkov, A.V., Karinski, Y.S. and Yankelevsky, D.Z. (2008b), "Internal blast loading in a buried lined tunnel", *Int. J. Impact Eng.*, **35**(3), 172-183. <https://doi.org/10.1016/j.ijimpeng.2007.01.001>.
- Gang, H. and Kwak, H.G. (2017), "A tensile criterion to minimize FE mesh-dependency in concrete beams under blast loading", *Comput. Concrete*, **20**(1), 1-10, <https://doi.org/10.12989/cac.2017.20.1.001>.
- Gupta, A.S. and Rao, K.S. (1998), "Index properties of weathered rocks: Inter-relationships and applicability", *Bull. Eng. Geology Environ.*, **57**(2), 161-172. <https://doi.org/10.1007/s100640050032>.
- H. Liu (2011), "Damage of cast-iron subway tunnels under internal explosions", *Proceedings of ASCE Geo-*

- Frontiers 2011*. Dallas, Texas.
- H.R. Yadav (2005), *Geotechnical Evaluation and Analysis of Delhi Metro Tunnels*, Ph.D Dissertation, Indian Institute of Technology Delhi, New Delhi, India.
- Hadianfard, M.A. and Farahani, A. (2012), "On the effect of steel columns cross sectional properties on the behaviours when subjected to blast loading", *Struct. Eng. Mech.*, **44**(4), 449-463. <https://doi.org/10.12989/sem.2012.44.4.449>.
- Hibbitt, D., Karlsson, B. and Sorensen, P. (2014), *ABAQUS User-Manual Release 6.14*. Dassault Systèmes Simulia Corp., Providence, RI.
- Higgins, W., Chakraborty, T. and Basu, D. (2012), "A high strain-rate constitutive model for sand and its application in finite element analysis of tunnels subjected to blast", *Int. J. Numer. Anal. Meth. Geomech.*, **37**(15), 2590-2610. <https://doi.org/10.1002/nag.2153>.
- J. Lee and G. Fenves (1998), "Plastic damage model for cyclic loading of concrete structures", *J. Eng. Mech.*, **124**(8), 892-900. [https://doi.org/10.1061/\(ASCE\)0733-9399\(1998\)124:8\(892\)](https://doi.org/10.1061/(ASCE)0733-9399(1998)124:8(892)).
- Jain, P. and Chakraborty, T. (2018), "Numerical analysis of tunnel in rock with basalt fiber reinforced concrete lining subjected to internal blast load", *Comput. Concrete*, **21**(4), 399-406, <https://doi.org/10.12989/cac.2018.21.4.399>.
- Kim, D.K., Ng, W.C.K. and Hwang, O. (2018), "An empirical formulation to predict maximum deformation of blast wall under explosion", *Struct. Eng. Mech.*, **68**(2), 237-245, <https://doi.org/10.12989/sem.2018.68.2.237>.
- Kim, S.H., Woo, H., Choi, G.G. and Yoon, K. (2018), "A new concept for blast hardened bulkheads with attached aluminum foam", *Struct. Eng. Mech.*, **65**(3), 243-250. <https://doi.org/10.12989/sem.2018.65.3.243>.
- Kumar, M., Goel, M.D., Matsagar, V.A. and Rao, K.S. (2015), "Response of semi-buried structures subjected to multiple blast loading considering soil-structure interaction", *Indian Geotech. J.*, **45**(3), 243-253. <https://doi.org/10.1007/s40098-014-0143-1>.
- Larcher, M. and Casadei, F. (2010), "Explosions in complex geometries-comparison of several approaches", European Commission, Joint Research Centre, Institute for Protection and Security of the Citizen, Italy
- Liang, Q., Li, J., Li, D. and Ou, E. (2013), 'Effect of blast-induced vibration from new railway tunnel on existing adjacent railway tunnel in Xinjiang, China', *Rock Mech. Rock Eng.*, **46**(1), 19-39. <https://doi.org/10.1007/s00603-012-0259-5>.
- Lublinter, J., Oliver, J., Oller, S. and Oñate, E. (1989) "A plastic damage model for concrete", *Int. J. Solids Struct.*, **25**(3), 299-329. [https://doi.org/10.1016/0020-7683\(89\)90050-4](https://doi.org/10.1016/0020-7683(89)90050-4).
- M. Larcher and F. Casadei (2010) "Explosions in Complex Geometries - A Comparison of Several Approaches", *Int. J. Protective Struct.*, **1**(2), 169-195. <https://doi.org/10.1260/2041-4196.1.2.169>.
- Ma, G.W., Hao, H. and Zhou, Y.X. (1998) "Modeling of wave propagation induced by underground explosion", *Comput. Geotech.*, **22**(3-4), 283-303, [https://doi.org/10.1016/S0266-352X\(98\)00011-1](https://doi.org/10.1016/S0266-352X(98)00011-1).
- Ma, G.W., Huang, X. and Li, J.C. (2009), "Damage assessment for buried structures against internal blast load", *Struct. Eng. Mech.*, **32**(2), 301-320, <https://doi.org/10.1007/s12209-008-0060-4>.
- Nam, J.W., Kim, H.J., Yi, N.H., Kim, I.S., Kim, J.H.J. and Choi, H.J. (2009), "Blast analysis of concrete arch structures for FRP retrofitting design", *Comput. Concrete*, **6**(4), 305-318. <https://doi.org/10.12989/cac.2009.6.4.305>.
- Nam, J.W., Yoon, I.S. and Yi, S.T. (2016), "Numerical evaluation of FRP composite retrofitted reinforced concrete wall subjected to blast load", *Comput. Concrete*, **17**(2), 215-225. <https://doi.org/10.12989/cac.2016.17.2.215>.
- Nateghi, R. (2012), "Evaluation of blast induced ground vibration for minimizing negative effects on surrounding structures", *Soil Dyn. Earthq. Eng.*, **43**, 133-138. <https://doi.org/10.1016/j.soildyn.2012.07.009>.
- Sadique, M.R., Ansari, M.I. and Athar, M.F. (2018), "Response study of concrete gravity dam against aircraft crash", *IOP Conference Series: Mater. Sci. Eng.*, **404**, 012027, <https://doi.org/10.1088/1757-899X/404/1/012027>.
- Tiwari, R., Chakraborty, T. and Matsagar, V. (2016a), "Dynamic analysis of a twin tunnel in soil subjected to

- internal blast loading”, *Indian Geotech. J.*, **46**(4), 369-380, <https://doi.org/10.1007/s40098-016-0179-5>.
- Tiwari, R., Chakraborty, T. and Matsagar, V. (2016b), “Dynamic analysis of tunnel in weathered rock subjected to internal blast loading”, *Rock Mech. Rock Eng.*, **49**(11), 4441-4458. <https://doi.org/10.1007/s00603-016-1043-8>.
- TM5-1300 (1990), *Structures to resist the effects of accidental explosions*. Technical Manual of the US Departments of the Army and Navy and the Air Force, U.S.A.
- Vehbi, O. (2018), “New methodology to prevent blasting damages for shallow tunnel”, *Geomech. Eng.*, **15**(6), 1227-1236. <https://doi.org/10.12989/gae.2018.15.6.1227>.
- Wahab, M.M. and Mazek, S.A. (2016), “Performance of double reinforced concrete panel against blast hazard”, *Comput. Concrete*, **18**(4) 807-826. <https://doi.org/10.12989/cac.2016.18.4.807>.
- Wang, W., Zhang, D., Lu, F., Wang, S.C. and Tang, F. (2013), “Experimental study and numerical simulation of the damage mode of a square reinforced concrete slab under close-in explosion”, *Eng. Fail. Anal.*, **27**, 41-51. <https://doi.org/10.1016/j.engfailanal.2012.07.010>
- Yang, Y., Xie, X. and Wang, R. (2010), “Numerical simulation of dynamic response of operating metro tunnel induced by ground explosion”, *J. Rock Mech. Geotech. Eng.*, **2**(4), 373-384. <https://doi.org/10.3724/SP.J.1235.2010.00373>
- Yuzhen H. and Huabei L. (2016), “Failure of circular tunnel in saturated soil subjected to internal blast loading”, *Geomech. Eng.*, **11**(3), 421-438. <https://doi.org/10.12989/gae.2016.11.3.421>.
- Zhao, C.F. and Chen, J.Y. (2013), “Damage mechanism and mode of square reinforced concrete slab subjected to blast loading”, *Theoretical Appl. Fracture Mech.*, **63-64**, 54-62, <https://doi.org/10.1016/j.tafmec.2013.03.006>.

